Published in final edited form as:

Cancer Res. 2009 April 1; 69(7): 3004–3012. doi:10.1158/0008-5472.CAN-08-3413.

Depletion of Guanine Nucleotides Leads to the Mdm2-Dependent Proteasomal Degradation of Nucleostemin

Min Huang[1], **Koji Itahana**[2], **Yanping Zhang**[2], and **Beverly S. Mitchell**[1]

[1]Department of Medicine, Divisions of Oncology and Hematology, and the Stanford Cancer Center, Stanford University, Palo Alto, California

[2]Lineberger Comprehensive Cancer Center, University of North Carolina at Chapel Hill, Chapel Hill, North Carolina

Abstract

Nucleostemin is a positive regulator of cell proliferation and is highly expressed in a variety of stem cells, tumors, and tumor cell lines. The protein shuttles between the nucleolus and the nucleus in a GTP-dependent fashion. Selective depletion of intracellular guanine nucleotides by AVN-944, an inhibitor of the *de novo* purine synthetic enzyme, IMP dehydrogenase, leads to the rapid disappearance of nucleostemin protein in tumor cell lines, an effect that does not occur with two other nucleolar proteins, nucleophosmin or nucleolin. Endogenous nucleostemin protein is completely stabilized by MG132, an inhibitor of the 26S proteasome, as are the levels of expressed enhanced green fluorescent protein–tagged nucleostemin, both wild-type protein and protein containing mutations at the G_1 GTP binding site. Nutlin-3a, a small molecule that disrupts the binding of the E3 ubiquitin ligase, Mdm2, to p53, stabilizes nucleostemin protein in the face of guanine nucleotide depletion, as does siRNA-mediated knockdown of Mdm2 expression and over-expression of a dominant-negative form of Mdm2. Neither Doxorubicin nor Actinomycin D, which cause the release of nucleostemin from the nucleolus, results in nucleostemin degradation. We conclude that nucleostemin is a target for Mdm2-mediated ubiquitination and degradation when not bound to GTP. Because this effect does not occur with other chemotherapeutic agents, the induction of nucleostemin protein degradation in tumor cells by IMP dehydrogenase inhibition or by other small molecules that disrupt GTP binding may offer a new approach to the treatment of certain neoplastic diseases.

Introduction

Nucleostemin (NS) is a multifunctional 62 kDa protein that was initially cloned from rat neuronal stem cells and identified as a GTP binding protein that contains two GTP consensus binding sites, a G4 site at codons 177-180 and G1 P loop binding site at codons 256-263 (1). NS is localized predominantly in the nucleolus, but as with many nucleolar proteins, shuttles to the nucleoplasm in response to cell cycle changes and to specific stress

Requests for reprints: Beverly S. Mitchell, Stanford Cancer Center, 800 Welch Road, Palo Alto, CA 94305-5796. Phone: 650-725-9621; Fax: 650-736-0607; bmitchell@stanford.edu..

Disclosure of Potential Conflicts of Interest

B.S. Mitchell: Unpaid consultant, Avalon Pharmaceuticals. The other authors disclosed no potential conflicts of interest.

conditions (1–5). It is highly expressed at both the RNA and protein levels in a number of tumor cell lines as well as in primary cancers and is more highly expressed in stem and progenitor cells than in differentiated cells (6, 7). The protein structure includes a highly basic NH_2-terminal region that has been identified as a direct p53 binding region (6). Reduction in the expression of NS using siRNAs or by heterozygous gene knockout experiments is associated with decreased cell proliferation and increased cellular senescence (8, 9). Homozygous knockouts in murine embryonic stem cells are lethal at embryonic d 3.5-5.5 (8). NS has thus been regarded as an important regulator of cell proliferation and is thought to be a direct transcriptional target of the c-*myc* protein (10–12).

Experiments in which GTP levels are reduced by 50% to 80% through inhibition of the *de novo* guanine nucleotide synthetic enzyme IMP dehydrogenase (IMPDH) have revealed that a number of nucleolar proteins are relocated to the nucleoplasm (1, 5), an event that has been termed the GTP-driven nucleolar cycle (2). Similar shifts of nucleolar proteins to the nucleoplasm also occur in response to DNA damage and to treatment of cells with chemotherapeutic agents such as doxorubicin. The nucleolus has thus been regarded as a sensor of cell stress (13), and the release of nucleolar proteins is causally related to an increase in p53 expression, with consequent induction of cell cycle arrest or apoptosis (14). A number of mechanisms have been proposed to mediate the p53 response, many of which seem to result from the displacement of the E3 ubiquitin ligase and tumor suppressor, Mdm2, from binding to p53, thus reducing the ubiquitination of p53 and its consequent destruction by the 26S proteasome. As one example, the nucleolar protein nucleophosmin or B23 upon leaving the nucleolus releases p14Arf that in turn displaces Mdm2 from p53 (15, 16). Similarly, the ribosomal proteins L5, L11, and L23 inhibit the Mdm2–mediated ubiquitination of p53 in response to ribosomal stress (17–19).

We have studied the role of the potent and specific IMPDH inhibitor, AVN944, in inducing nucleolar stress. Previous data have shown that the decrease in GTP levels induced by this drug causes an egress of nucleolar proteins that is associated with inhibition of pre rRNA synthesis and is completely reversible with GTP repletion. This effect is also associated with a significant increase in both p53 and p14Arf expression and is analogous to the effects induced by low dose Actinomycin D, an inhibitor of RNA polymerase I (5). In addition, however, we have recently found that NS is rapidly degraded after GTP depletion in striking contrast to other nucleolar proteins. We now present data supporting a role for Mdm2 in ubiquitinating NS in the GTP-unbound state and targeting it for proteasomal degradation. Modulation of the binding of GTP to NS presents an important new avenue toward reducing its expression in tumor cells at the protein level and differentiates GTP-depleting agents such as AVN944 from other chemotherapeutic drugs that do not have this effect.

Materials and Methods

Cell culture conditions and reagents used

U2OS, MCF-7, NB4, and K562 cells were grown in DMEM or RPMI 1640 supplemented with 10% fetal bovine serum (HyClone; PERBIO) and 100 U/mL of penicillin and streptomycin. Actinomycin-D, Nutlin-3a, and Adriamycin were obtained from EMD Chemicals, Inc. 4’,6-Diamino-2-phenylindol (DAPI) was purchased from Molecular Probes,

Inc. Mouse monoclonal anti-nucleolin (MS-3), anti-p53 (DO-1), and anti-HA probe (F-7) antibodies and protein A/G PLUS-Agarose were from Santa Cruz Biotechnology. Rabbit polyclonal anti-NPM was from Cell Signaling Technology Inc. Goat Anti-Nucleostemin Polyclonal Antibody was from R&D Systems, Inc. Anti-actin monoclonal antibody was from Sigma. Full-Length A.v. Polyclonal EGFP Antibody was from Clontech Laboratories, Inc. Fluorescein (FITC)-conjugated donkey anti-rabbit F(ab')2 and rhodamine-conjugated goat anti-mouse secondary antibodies were purchased from Jackson ImmunoResearch.

RNA isolation, cDNA synthesis, and construction of enhanced green fluorescent protein–tagged NS

Total RNAs were extracted from U2OS cells with Trizol reagent (Invitrogen) following the manufacturer's instruction. Two micrograms of total RNA were used for first-strand cDNA synthesis using oligo (dT) as a primer for SuperScript II RNase H Reverse Transcriptase (SuperScript First-Strand Synthesis System for RT-PCR; Invitrogen). One tenth of the resulting first-strand cDNA was then used for PCR amplification with high-fidelity pfx DNA polymerase (Invitrogen). The primers for amplifying the entire coding sequence of NS are listed in Table 1. The italicized bases are the restriction enzyme sites (Xho1 and BamH1) with four extra bases added at each end to promote efficient digestion by the restriction enzymes. cDNAs of NS amplified as above were cloned into Xho1 and BamH1 site of p-EGFP-C3 (BD; biotech), and the resulting plasmids were sequenced.

Mutagenesis of enhanced green fluorescent protein–NS, transient and stable transfection, and fluorescence-activated cell sorting

G261V and G261V plus G266V mutants of NS were created using the Stratagene QuikChange mutagenesis kit (Stratagene). The wild-type enhanced green fluorescent protein (EGFP)-NS construct and its GTP-binding site mutants were transiently introduced into U2OS cells by Superfect transfection reagent (Qiagen) according to the manufacturer's instruction. Twenty-four hours after transfection, the U2OS cells transfected with wild-type EGFP-NS were subjected to G418 selection (1 mg/mL) for 2 wk, and the EGFP-positive cells were then isolated by FACStar plus sorting (Becton Dickinson). Postsorting, the cells stably expressing EGFP-NS were collected and grown in cell growth medium.

Semiquantitative reverse transcription-PCR

RNA isolation and cDNA synthesis were conducted as described above. One tenth of the resulting first-strand cDNA was then used for PCR amplification. Different sets of primers were designed and synthesized for PCR analysis. The primer pairs used for amplifying human NS and cyclin-B1 are listed in Table 1. PCR products were analyzed by 1% agarose gel and visualized by staining with ethidium bromide.

Immunocytochemistry

U2OS cells were transiently transfected with EGFP-NS constructs (wild-type, G261V, and G261V plus G266V). Twenty-four hours after transfection, cells were grown on coverslips in 24-well plates in DMEM complete medium for 12 h and then treated with AVN-944 (1 μmol/L) or vehicle control in the presence or absence of MG132 (5 μmol/L) for 8 h. In other

experiments, U2OS cells stably expressing EGFP-NS were pretreated with nutlin-3a (10 μmol/L) for 24 h, and then exposed to AVN-944 (1 μmol/L), Act-D (5 nmol/L), or doxorubicin (1 μmol/L) for an additional 16 h. The cells were fixed in 4% PBS-paraformaldehyde solution for 20 min followed by permeabilization with 0.1% Triton X-100 in PBS for 15 min. After blocking with 5% bovine serum albumin (BSA) in PBS for 30 min, coverslips were inverted onto a 30-μL drop of the primary antibodies diluted in PBS containing 0.1% Triton-X-100 and 5% BSA (1:50 for NPM, nucleolin, and nucleostemin). After 1-h incubation with antibody and subsequent washing with PBS ×3 (10 min each), coverslips were inverted again onto 30-μL drops of the secondary antibodies diluted in PBS containing 5% BSA and 0.1% Triton-X 100 [rhodamine-congugated secondary antibody (1:300); FITC-conjugated secondary antibody (1:50)]. After washing, coverslips were stained with DAPI (300 nmol/L) for 5 min, washed with PBS ×3 (5 min each), mounted in Gel Mount Aqueous Mounting Medium (Sigma-Chemical Co.) and examined by fluorescent microscopy.

Western blotting

Protein lysates were prepared as described previously (5). For immunoblotting, 20 μg of protein lysate were electrophoresed on SDS-PAGE gels and transferred to polyvinylidene difluoride membrane (Immobilon-P; Millipore). Specific antigens were probed using the corresponding primary antibody, followed by horseradish peroxidase–conjugated secondary antibody. Western blots were visualized using enhanced chemiluminescence (Chemiluminescence Reagent Plus; Perkin-Elmer Life Sciences).

Amaxa electroporation of Mdm2 double-stranded RNA (siRNA)

Mdm2 siRNA targeting nucleotide 627 to 647 (5′-AATCAGCAGGAATCATCGGAC-3′) and a scrambled control oligonucleotide (5′-AAAGTCATCGTGACTACGACG-3′) were described previously (20). The oligonucleotides were synthesized by Qiagen, and electroporated into U2OS cells by using Amaxa Electroporation kit V (Amaxa) according to the manufacturer's instruction. Briefly, 5×10^6 cells per sample were resuspended in 100 μL of room temperature Nucelofector solution and then electroporated into U2OS cells using 200 or 400 pmol of Mdm2 siRNA, scrambled control-siRNA or a mock control (Program X-001 on the Amaxa Nucleofector Device). Forty-eight hours after electroporation, cells were exposed to 1 μmol/L AVN944 or vehicle control for additional 16 h, and then analyzed by flow cytometry. Knockdown of Mdm2 was measured by immunoblot analysis 24 or 48 h posttransfection. Actin was used as a loading control.

Flow cytometry

Cells were harvested by trypsinization and washed with PBS. The cells were resuspended at 2×10^6 cells per mL in PBS and analyzed by Flow cytometric analysis (FACS Calibur; Becton Dickinson). In all cases, parental U2OS cells or U2OS cells transfected with scrambled control-siRNA were used as negative controls.

Results

GTP-depletion induces selective reduction of NS protein levels

Two cell lines, MCF-7 and NB4, were treated with 1 μmol/L AVN944 and cells were harvested at 2-hour intervals for time periods up to 24 hours. Western blot analysis showed that nucleostemin protein was reduced at 4 hours and nearly absent at 8 hours in both cell lines, whereas nucleophosmin and nucleolin protein levels were unchanged (Fig. 1*A* and *B*). The AVN944-induced degradation of NS was completely prevented by pretreatment of cells with 50 μmol/L guanosine (data not shown). In addition, the AVN-944–induced degradation of NS was reversed by withdrawal of AVN-944 and by the subsequent addition of guanosine to replete GTP pools through the hypoxanthine-guanine phosphoribosyltransferase pathway (21) in the presence of AVN-944 (Fig. 1*C*). These results show that the AVN944-induced degradation of NS is dependent on GTP levels. To determine whether this effect occurs at the transcriptional level, reverse transcription-PCR (RT-PCR) was performed using two different primer sets directed at exons 1 to 6 (NS1) and exons 8 to 11 (NS2) in MCF-7 cells. Cyclin-B1 levels were used as an internal control. As shown in Fig. 1*D*, levels of mRNA were unchanged for NS over this time period, supporting posttranscriptional regulation. We next asked whether the reduction in NS protein levels could be rescued by treatment of cells with the proteasome inhibitor MG132. As shown in Fig. 2*A* and *B*, MG132 almost completely prevented the loss of NS protein at 24 hours in U2OS and K562 cell lines and partially reversed the loss in MCF-7 cells at 24 hours. The preventive effect of MG132 on NS degradation was observed at concentrations of AVN-944 up to 10 μmol/L (Fig. 2*C*), >10-fold higher than the IC_{50} of the drug for this cell line. These results suggest that NS levels are controlled by proteasome-mediated degradation.

Proteasome inhibition prevents AVN-944–induced translocation of NS and nucleolin

Because inhibition of IMPDH and subsequent nucleotide depletion has been directly associated with the nucleolar “stress response,” we also examined the effect of MG132 on the alteration in nucleolar protein distribution associated with AVN944 treatment. As shown in Fig. 3, AVN944 induces translocation of NS and nucleolin from the nucleolus into the nucleus, as shown in panel 3 (Fig. 3*A*). The addition of MG132 results in nucleolar retention of NS and, to a lesser extent, nucleolin. Of particular interest is the observation that mutation of human NS (NM_014366 in the National Center for Biotechnology Information nucleotide database) at the GTP G1 binding site (G261V and the G261V+G266V double mutant) also results in nucleoplasmic localization, as has been shown previously (1), and MG132 also localizes these mutated proteins to the nucleolus (Fig. 3*B*). Previous data have shown that the t1/2 of the protein mutated at the G_1 binding site is reduced and that this mutation may act as a dominant negative in inducing cell death (6). Additional data (data not shown) obtained on EGFP-labeled protein expressed in U2OS cells show that MG-132 enhances the stability of the protein mutated at the G_1 site. These data provide further evidence that GTP binding protects NS from degradation through proteasome-mediated degradation.

NS is a target of Mdm2-dependent degradation

We then asked whether Mdm2 might be responsible for NS ubiquitination and subsequent proteasomal degradation. This hypothesis was further suggested by the very recent finding

that NS binds to Mdm2, as well as to p53 (22). We therefore examined the effect of Nutlin-3a, a molecule that specifically binds to the p53 binding site of Mdm2 (23), on NS stability. Figure 4*A* and *B* show that Nutlin-3a markedly enhances the stability of EGFP-tagged NS expressed in U2OS cells, as shown by flow cytometric analysis. A similar experiment performed in the absence and presence of AVN-944 (Fig. 4*C*) shows significantly enhanced fluorescence intensity resulting from nutlin-3a treatment for both control and AVN-944-treated cells. Western blot analysis (Fig. 4*D*) confirms that AVN944-induced degradation of NS is abrogated in the presence of Nutlin-3a. As we have previously shown (5), AVN-944 treatment causes the accumulation of p53, as does Nutlin-3a (Fig. 4*D*). However, treatment of cells with Nutlin-3a alone does not induce the degradation of NS (Fig. 4*D*), suggesting that the accumulation of p53 is not causally related to NS degradation. In addition, we have found that AVN-944 induces the degradation of NS in both Raji B cells containing p53 mutations (213 Arg→Gln and 234 His→Tyr; ref. 24) and p53-null SaoS2 osteosarcoma cells (data not shown; ref. 25). We conclude that p53 activity is not required for NS degradation.

To confirm that Mdm2 is responsible for NS degradation, we asked whether a reduction in Mdm2 expression would increase NS stability. A knockdown of Mdm2 expression using 400 pmol of siRNA for 48 hours increased the levels of both endogenous and EGFP-tagged NS, although it did not restore them to control levels (Fig. 5*A*). In addition, we compared the effects on NS stability of expressing either wt-Mdm2 or Mdm2 containing a C464A mutation that inactivates the E3 ubiquitin ligase activity and serves as a dominant-negative, stabilizing Mdm2 substrates including p53 and the androgen receptor (26, 27). As shown in Fig. 5*B*, overexpression of wt-Mdm2 results in mildly reduced fluorescence intensity of EGFP-NS compared with control-transfected cells. In contrast, overexpression of C464A-Mdm2 led to a shift toward increased fluorescence intensity (Fig. 5*C*), supporting a small dominant-negative effect on NS degradation. In addition, in data not shown, overexpression of wt-Mdm2 markedly enhanced the degradation of NS induced by AVN-944, whereas overexpression of the E3 ligase mutant decreased degradation.

Inhibition of Mdm2 by Nutlin-3a prevents the translocation of NS, nucleophosmin, and nucleolin induced by AVN944

Finally, we determined that nutlin-3a pretreatment relocalized NS and nucleolin to the nucleolus (Fig. 6*A*), while enhancing the expression of both Mdm2 and p53 in the nucleus (Fig. 6*B*). Importantly, the nucleoplasmic localization of NS and nucleolin induced by Doxorubicin and by low-dose Actinomycin D, an inhibitor of RNA polymerase I, was not reversible with nutlin-3a (Fig. 6*C* and *D*). These data support the conclusion that inhibition of the Mdm2-p53 interaction by nutlin-3a has a specific effect on preventing the degradation of NS induced by GTP depletion and that the nucleoplasmic localization itself is insufficient to account for NS instability.

We therefore propose a model in which a reduction in GTP levels induced by IMPDH inhibition results in NS leaving the nucleolus as a result of reduced binding of GTP to the protein. The resultant conformational change facilitates binding to the acidic domain of Mdm2. This interaction interferes with the binding of p53 to Mdm2, resulting in p53 up-

regulation. NS is then ubiquitinated by Mdm2 and targeted to the 26S proteasome for degradation. This model will require further testing using *in vitro* assay systems.

Discussion

Depletion of intracellular ribonucleotides was first shown to induce a reversible G_0-G_1 cell cycle arrest associated with the prolonged induction of p53 and the Cdk inhibitor $p21^{Waf1/Cip1}$ by Linke and colleagues (28). However, the mechanism by which p53 was activated was not well-understood at that time. More recently, the specific depletion of guanine ribonucleotides using inhibitors of the enzyme IMPDH has been shown to cause nucleolar disruption and the release of nucleolar proteins into the nucleoplasm, the so-called GTP-driven nucleolar cycle (1). IMPDH is the rate-limiting enzyme in the *de novo* synthetic pathway for guanine nucleotides, and inhibitors of this enzyme are effective immunosuppressive agents, as well as potential chemotherapeutic and antiviral drugs; the potent and specific inhibitor AVN944 is currently in phase I trials for the treatment of refractory hematologic malignancies. The release of nucleolar proteins by IMPDH inhibitors could thus be quite relevant to their mechanism of action. Of the nucleolar proteins studied to date, an increasing number including p14Arf and the ribosomal proteins L11, L5, and L23 have been shown to displace the E3 ubiquitin ligase Mdm2 from p53, resulting in decreased p53 ubiquitin-dependent proteasomal degradation and increased p53 protein levels (17, 18, 29–34). Thus, depletion of ribonucleotides, and of GTP in particular, may well cause an increase in p53 levels at least in part through this mechanism.

We have determined that the dramatic reduction in NS protein levels is mediated by proteasomal degradation of NS. NS has recently been shown to bind to Mdm2 (22). Using Nutlin-3a to bind to the acidic binding domain of Mdm2, the site of both p53 and NS binding to Mdm2, we found that NS protein levels were greatly stabilized, strongly implicating Mdm2 ubiquitin ligase activity as at least one mediator of NS instability. Further support for this conclusion comes from the enhancement of NS degradation by the expression of wt Mdm2 and stabilization with the expression of a dominant-negative Mdm2 mutant. These data, together with the evidence that disruption of GTP binding to NS at the G_1 binding site also leads to NS instability and is also rescued by MG132, lead to the conclusion that a conformational change in NS induced by the release of GTP increases the susceptibility of the protein to ubiquitination by Mdm2 and its subsequent proteasomal degradation. Although we were unable to obtain truly reproducible evidence of NS ubiquitination using HA-tagged ubiquitin in immunoprecipitation experiments, the preponderance of evidence strongly supports a short-lived ubiquitinated intermediate. Similar difficulty has been encountered in demonstrating ubiquitinated p53 under similar conditions (35). It is possible that the proteolysis of NS contributes to the induction of apoptosis by IMPDH inhibitors, suggesting a mechanism of action that is distinct from those of other chemotherapeutic inducers of cell stress. NS depletion through siRNA treatment activates p53 and increases the levels of Mdm2, a p53 target gene (22, 36). In addition, however, there are clearly p53-independent effects of loss of NS, as shown by the failure of p53-deficient cells to rescue the proliferative defect of NS–/– blastocysts (8). Thus, the reduction in NS protein levels that occurs with IMPDH inhibition should have broader effects than p53 induction, consistent with the ability of NS siRNA to inhibit the growth of

p53-deficient cells. The fact that NS degradation does not occur with other chemotherapeutic drugs that induce “nucleolar stress” suggests that there may be a unique effect on cell growth and/or apoptosis that results from IMPDH inhibition and GTP depletion. The question of whether the cellular response to NS degradation is tumor cell–specific remains to be determined, but the increased expression of NS in tumor cells and cell lines suggests that tumor cells may be more dependent on NS for survival than are normal cells.

The binding of Nutlin-3a to Mdm2 causes a conformational change in Mdm2 (37), further blocking the binding of NS to Mdm2 and leading to its accumulation. We recognize, however, that other ubiquitin ligases may also be involved. In the case of p53, for example, E3 ligases including p53-induced protein with RING-H2 domain (PIRH2), constitutively photomorphogenic 1 (COP1), and ADP ribosylation factor–binding protein 1 (SRF-BP1) have also been identified as p53 ubiquitin ligases (38–40). It was proposed that these distinct E3 ligases may be involved in the differential regulation of p53 stability under diverse stress conditions or in different tissues (41). However, a dominant role of Mdm2 as a regulator of NS levels, even in the absence of GTP depletion, is supported by our data.

Finally, we have made the observation that Nutlin-3a pretreatment stabilizes the nucleolus against the release of nucleophosmin and nucleolin into the nucleoplasm, although neither of these proteins seems to be a substrate for proteasomal degradation. Taken together with the observations that mutations within the GTP binding site result in the nucleoplasmic localization of the NS and that MG132 treatment also stabilizes the localization of NS and nucleolin in the nucleolus, it is possible that the Mdm2-mediated ubiquitination of NS plays an important role in regulating the trafficking of other nucleolar proteins between the nucleolar and nucleoplasmic compartments. Intracellular GTP levels could therefore be pivotal in the Mdm2-dependent regulation of nucleolar protein localization.

Acknowledgments

Grant support: NIH grant 5R01-CA064192 (B.S. Mitchell) and by a Translational Research Award (B.S. Mitchell) from the Leukemia and Lymphoma Society.

The costs of publication of this article were defrayed in part by the payment of page charges. This article must therefore be hereby marked *advertisement* in accordance with 18 U.S.C. Section 1734 solely to indicate this fact.

References

1. Tsai RY, McKay RD. A multistep, GTPdriven mechanism controlling the dynamic cycling of nucleostemin. J Cell Biol. 2005; 168:179–84. [PubMed: 15657390]
2. Misteli T. Going in GTP cycles in the nucleolus. J Cell Biol. 2005; 168:177–8. [PubMed: 15657389]
3. Meng L, Yasumoto H, Tsai RY. Multiple controls regulate nucleostemin partitioning between nucleolus and nucleoplasm. J Cell Sci. 2006; 119:5124–36. [PubMed: 17158916]
4. Meng L, Zhu Q, Tsai RY. Nucleolar trafficking of nucleostemin family proteins: common versus protein-specific mechanisms. Mol Cell Biol. 2007; 27:8670–82. [PubMed: 17923687]
5. Huang M, Ji Y, Itahana K, Zhang Y, Mitchell B. Guanine nucleotide depletion inhibits pre-ribosomal RNA synthesis and causes nucleolar disruption. Leuk Res. 2008; 32:131–41. [PubMed: 17462731]

6. Tsai RY, McKay RD. A nucleolar mechanism controlling cell proliferation in stem cells and cancer cells. Genes Dev. 2002; 16:2991–3003. [PubMed: 12464630]
7. Han C, Zhang X, Xu W, Wang W, Qian H, Chen Y. Cloning of the nucleostemin gene and its function in transforming human embryonic bone marrow mesenchymal stem cells into F6 tumor cells. Int J Mol Med. 2005; 16:205–13. [PubMed: 16012751]
8. Beekman C, Nichane M, De Clercq S, et al. Evolution-arily conserved role of nucleostemin: controlling proliferation of stem/progenitor cells during early vertebrate development. Mol Cell Biol. 2006; 26:9291–301. [PubMed: 17000755]
9. Zhu Q, Yasumoto H, Tsai RY. Nucleostemin delays cellular senescence and negatively regulates TRF1 protein stability. Mol Cell Biol. 2006; 26:9279–90. [PubMed: 17000763]
10. Dave SS, Fu K, Wright GW, et al. Molecular diagnosis of Burkitt's lymphoma. N Engl J Med. 2006; 354:2431–42. [PubMed: 16760443]
11. Rosenwald A, Wright G, Chan WC, et al. The use of molecular profiling to predict survival after chemotherapy for diffuse large-B-cell lymphoma. N Engl J Med. 2002; 346:1937–47. [PubMed: 12075054]
12. Shaffer AL, Wright G, Yang L, et al. A library of gene expression signatures to illuminate normal and pathological lymphoid biology. Immunol Rev. 2006; 210:67–85. [PubMed: 16623765]
13. Boisvert FM, van Koningsbruggen S, Navascues J, Lamond AI. The multifunctional nucleolus. Nat Rev Mol Cell Biol. 2007; 8:574–85. [PubMed: 17519961]
14. Mayer C, Grummt I. Cellular stress and nucleolar function. Cell Cycle. 2005; 4:1036–8. [PubMed: 16205120]
15. Korgaonkar C, Hagen J, Tompkins V, et al. Nucleophosmin (B23) targets ARF to nucleoli and inhibits its function. Mol Cell Biol. 2005; 25:1258–71. [PubMed: 15684379]
16. Bertwistle D, Sugimoto M, Sherr CJ. Physical and functional interactions of the Arf tumor suppressor protein with nucleophosmin/B23. Mol Cell Biol. 2004; 24:985–96. [PubMed: 14729947]
17. Jin A, Itahana K, O'Keefe K, Zhang Y. Inhibition of HDM2 and activation of p53 by ribosomal protein L23. Mol Cell Biol. 2004; 24:7669–80. [PubMed: 15314174]
18. Zhang Y, Wolf GW, Bhat K, et al. Ribosomal protein L11 negatively regulates oncoprotein MDM2 and mediates a p53-dependent ribosomal-stress checkpoint pathway. Mol Cell Biol. 2003; 23:8902–12. [PubMed: 14612427]
19. Dai MS, Zeng SX, Jin Y, et al. Ribosomal protein L23 activates p53 by inhibiting MDM2 function in response to ribosomal perturbation but not to translation inhibition. Mol Cell Biol. 2004; 24:7654–68. [PubMed: 15314173]
20. Carroll VA, Ashcroft M. Regulation of angiogenic factors by HDM2 in renal cell carcinoma. Cancer Res. 2008; 68:545–52. [PubMed: 18199551]
21. Sidi Y, Hudson JL, Mitchell BS. Effects of guanine ribonucleotide accumulation on the metabolism and cell cycle of human lymphoid cells. Cancer Res. 1985; 45:4940–5. [PubMed: 2411392]
22. Dai MS, Sun XX, Lu H. Aberrant expression of nucleostemin activates p53 and induces cell cycle arrest via inhibition of MDM2. Mol Cell Biol. 2008; 28:4365–76. [PubMed: 18426907]
23. Vassilev LT, Vu BT, Graves B, et al. In vivo activation of the p53 pathway by small-molecule antagonists of MDM2. Science. 2004; 303:844–8. [PubMed: 14704432]
24. Lapalombella R, Zhao X, Triantafillou G, et al. A novel Raji-Burkitt's lymphoma model for preclinical and mechanistic evaluation of CD52-targeted immuno-therapeutic agents. Clin Cancer Res. 2008; 14:569–78. [PubMed: 18223233]
25. Issaeva N, Friedler A, Bozko P, Wiman KG, Fersht AR, Selivanova G. Rescue of mutants of the tumor suppressor p53 in cancer cells by a designed peptide. Proc Natl Acad Sci U S A. 2003; 100:13303–7. [PubMed: 14595027]
26. Katayama H, Sasai K, Kawai H, et al. Phosphorylation by aurora kinase A induces Mdm2-mediated destabilization and inhibition of p53. Nat Genet. 2004; 36:55–62. [PubMed: 14702041]
27. Lin HK, Wang L, Hu YC, Altuwaijri S, Chang C. Phosphorylation-dependent ubiquitylation and degradation of androgen receptor by Akt require Mdm2 E3 ligase. EMBO J. 2002; 21:4037–48. [PubMed: 12145204]

28. Linke SP, Clarkin KC, Di Leonardo A, Tsou A, Wahl GM. A reversible, p53-dependent G0/G1 cell cycle arrest induced by ribonucleotide depletion in the absence of detectable DNA damage. Genes Dev. 1996; 10:934–47. [PubMed: 8608941]
29. Lohrum MA, Ludwig RL, Kubbutat MH, Hanlon M, Vousden KH. Regulation of HDM2 activity by the ribosomal protein L11. Cancer Cell. 2003; 3:577–87. [PubMed: 12842086]
30. Dai MS, Lu H. Inhibition of MDM2-mediated p53 ubiquitination and degradation by ribosomal protein L5. J Biol Chem. 2004; 279:44475–82. [PubMed: 15308643]
31. Dai MS, Zeng SX, Jin Y, Sun XX, David L, Lu H. Ribosomal protein L23 activates p53 by inhibiting MDM2 function in response to ribosomal perturbation but not to translation inhibition. Mol Cell Biol. 2004; 24:7654–68. [PubMed: 15314173]
32. Dai MS, Shi D, Jin Y, et al. Regulation of the MDM2–53 pathway by ribosomal protein L11 involves a post-ubiquitination mechanism. J Biol Chem. 2006; 281:24304–13. [PubMed: 16803902]
33. Lindstrom MS, Jin A, Deisenroth C, Wolf GW, Zhang Y, Xiong Y. Cancer-associated mutations in MDM2 zinc finger domain disrupt ribosomal protein interaction and attenuate MDM2-induced p53 degradation. Mol Cell Biol. 2007; 27:1056–68. [PubMed: 17116689]
34. Lindstrom MS, Deisenroth C, Zhang Y. Putting a finger on growth surveillance: insight into MDM2 zinc finger-ribosomal protein interactions. Cell Cycle. 2007; 6:434–7. [PubMed: 17329973]
35. Maki CG, Huibregtse JM, Howley PM. In vivo ubiquitination and proteasome-mediated degradation of p53. Cancer Res. 1996; 56:2649–54. [PubMed: 8653711]
36. Ma H, Pederson T. Depletion of the nucleolar protein nucleostemin causes G1 cell cycle arrest via the p53 pathway. Mol Biol Cell. 2007; 18:2630–5. [PubMed: 17494866]
37. Wallace M, Worrall E, Pettersson S, Hupp TR, Ball KL. Dual-site regulation of MDM2 E3-ubiquitin ligase activity. Mol Cell. 2006; 23:251–63. [PubMed: 16857591]
38. Leng RP, Lin Y, Ma W, et al. Pirh2, a p53-induced ubiquitin-protein ligase, promotes p53 degradation. Cell. 2003; 112:779–91. [PubMed: 12654245]
39. Dornan D, Wertz I, Shimizu H, et al. The ubiquitin ligase COP1 is a critical negative regulator of p53. Nature. 2004; 429:86–92. [PubMed: 15103385]
40. Chen D, Kon N, Li M, Zhang W, Qin J, Gu W. ARFBP1/Mule is a critical mediator of the ARF tumor suppressor. Cell. 2005; 121:1071–83. [PubMed: 15989956]
41. Vassilev LT. MDM2 inhibitors for cancer therapy. Trends Mol Med. 2007; 13:23–31. [PubMed: 17126603]

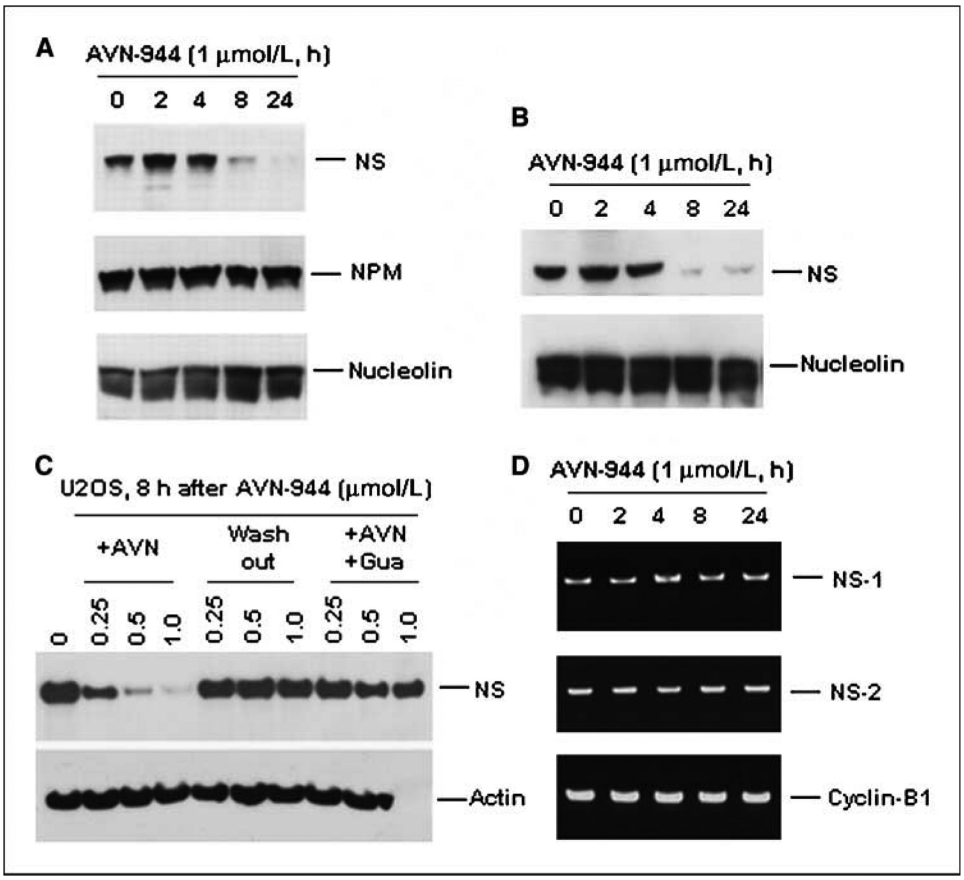

Figure 1.

Effect of AVN-944 on nucleostemin protein and mRNA levels in two cell lines. *A*, MCF-7 and (*B*) NB4 cells were exposed to 1 μmol/L AVN-944 for the times indicated. Cells were lysed as described in Materials and Methods, and 20 μg of total protein were loaded for immunoblot analysis for NS, nucleophosmin (*NPM*), or nucleolin; *C*, U2OS cells were first treated with AVN-944 at the concentrations indicated for 8 h, then either washed thrice and grown in fresh medium for an additional 16 h or continuously exposed to AVN-944 in the presence or absence of 50 μmol/L guanosine for 16 h. Total protein (30 μg) were loaded for immunoblot analysis of NS and actin. *D*, levels of mRNA expression of NS (NS-1 and NS-2 used two sets of primers) and cyclin-B1 in MCF-7 cells were determined by RT-PCR.

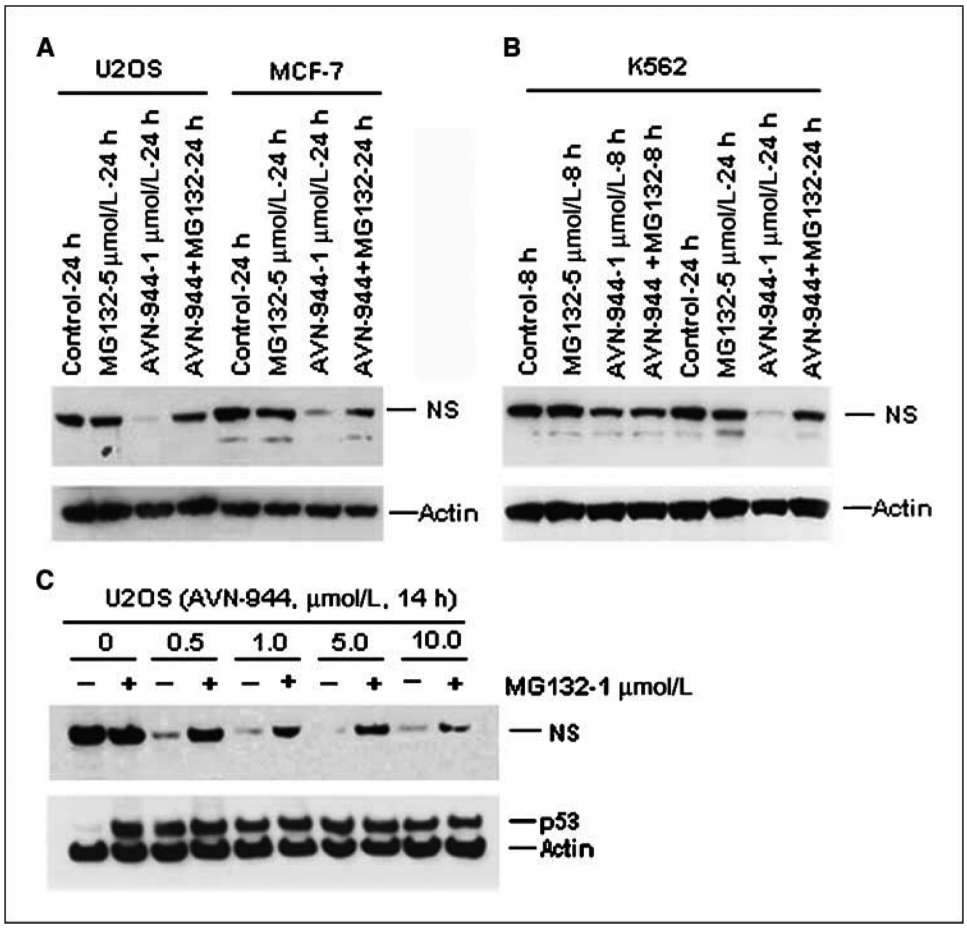

Figure 2.

AVN-944–induced degradation of NS is inhibited by MG132 treatment in multiple cell lines. *A*, U2OS, MCF-7, and (*B*) K562 cells were treated with 1 μmol/L AVN-944 in the absence or presence of 5 μmol/L MG132 for 8 or 24 h. Cells were then lysed as described in Materials and Methods, and 20 μg of total protein were loaded for immunoblot analysis for NS and actin. *C*, U2OS cells were treated with AVN-944 at doses indicated in the absence or presence of 1 μmol/L MG132 for 14 h. Cells were then lysed and 20 μg of total protein were loaded for immunoblot analysis for NS, p53, and actin.

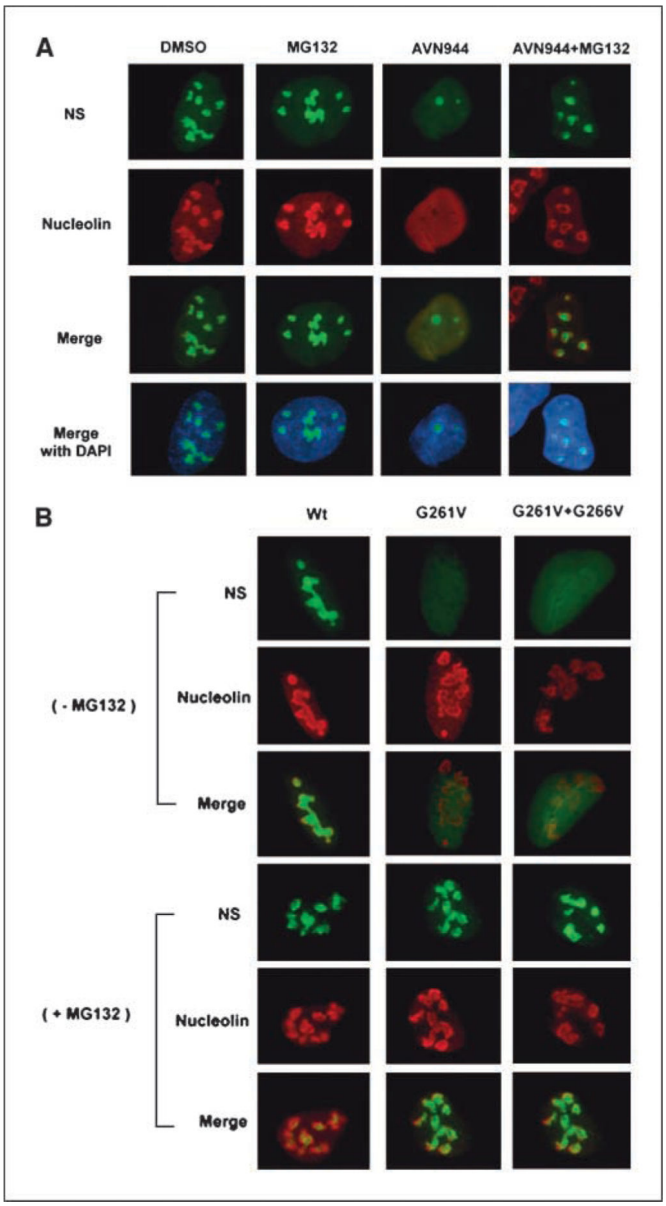

Figure 3.

MG132 treatment prevents AVN-944–induced translocation of NS and nucleolin and relocates GTP binding mutants of NS from the nucleoplasm to the nucleolus. *A*, U2OS cells were treated with 1 μmol/L AVN-944 in the absence or presence of 5 μmol/L MG132 for 8 h. *B*, U2OS cells were transiently transfected with wild-type or two NS constructs mutated at the G_1 binding site. Twenty-four hours after transfection, cells were treated with 5 μmol/L MG132 for 8 h. Cells were fixed, permeabilized, stained for nucleolin and nucleostemin, as described in Materials and Methods, and observed using fluorescent microscopy at ×100 magnification.

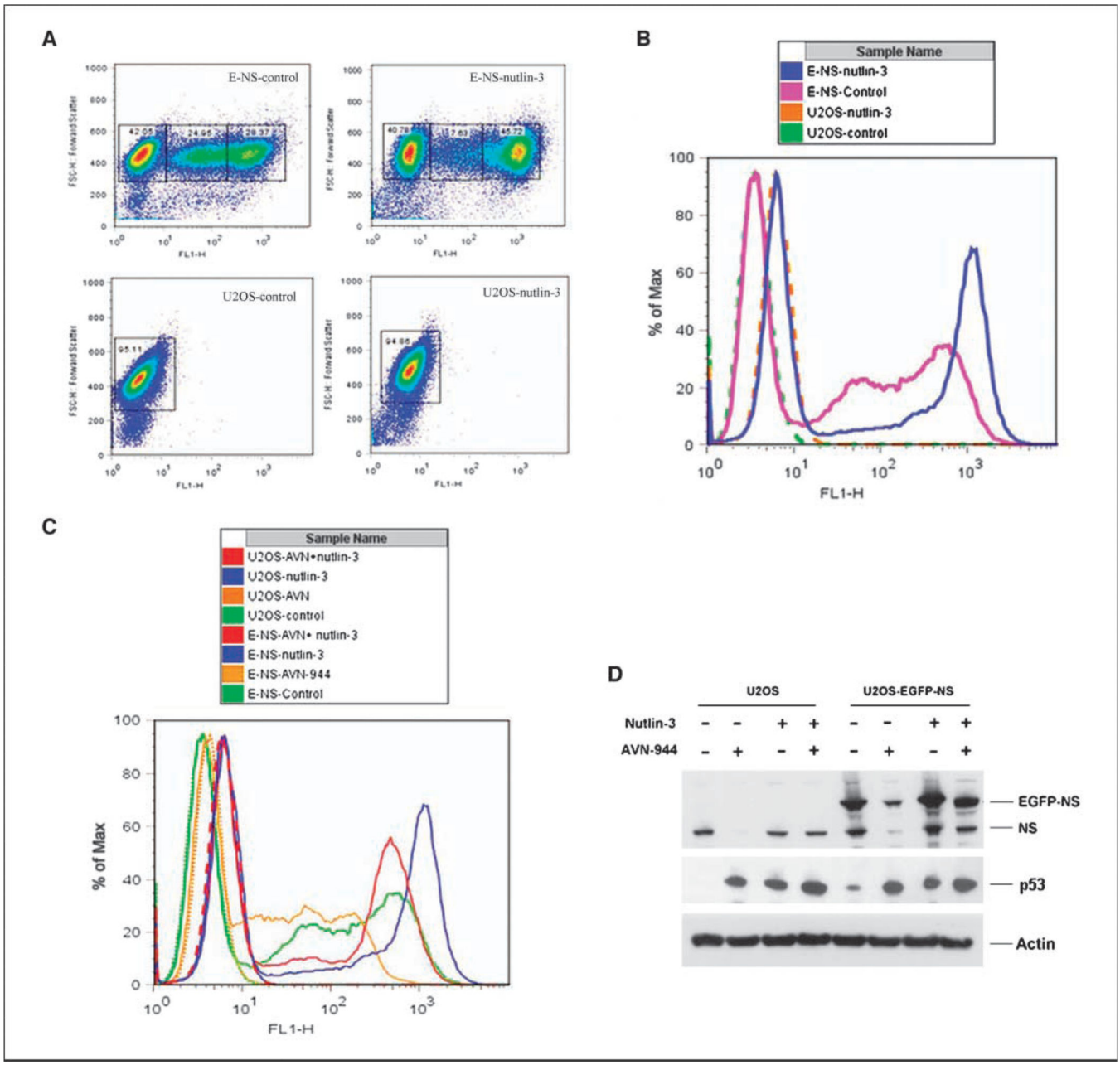

Figure 4.

Effects of nutlin-3a on the stability of nucleostemin in U2OS cells stably expressing EGFP-NS. U2OS cells and U2OS cells stably expressing EGFP-NS were pretreated with 10 μmol/L nutlin-3a for 24 h, then exposed to 1 μmol/L AVN-944 or vehicle control for an additional 16 h. Quantitative assessment of EGFP-NS protein was performed by flow cytometry, and shown as a (*A*) dot plot and (*B* and *C*) histogram. In the dot plot, the plot is gated according to the fluorescent intensity [the FL1-height (*FL1-H*)] of the EGFP-tagged NS. In U2OS cells expressing EGFP-NS, ~40% of the total cell population are EGFP-negative or contain undetectable level of EGFP-NS. *B*, the parental U2OS control cells with (*green fine dashed lines*) or without (*brown fine dashed lines*) nutlin-3a, respectively; the

EGFP-expressing U2OS cells in the absence (*pink heavy solid lines*) or presence (*blue heavy solid lines*) of nutlin-3a, respectively. *C*, control EGFP-NS–expressing U2OS cells in the absence (*green fine solid lines*) or presence (*blue fine solid lines*) of nutlin-3a, respectively; the AVN-944–treated EGFP-NS–expressing U2OS cells in the absence (*brown fine solid lines*) or presence (*red fine solid lines*) of nutlin-3a, respectively; the control EGFP-NS expressing U2OS cells in the absence (*green fine dashed lines*) or presence (*blue fine dashed lines*) of Nutlin-3a, respectively; the AVN-944–treated EGFP-NS expressing U2OS cells in the absence (*brown fine dashed lines*) or presence (*red fine dashed lines*) of nutlin-3a, respectively. *D*, Western blot of endogenous NS, p53, and EGFP-NS with or without nutlin-3a treatment.

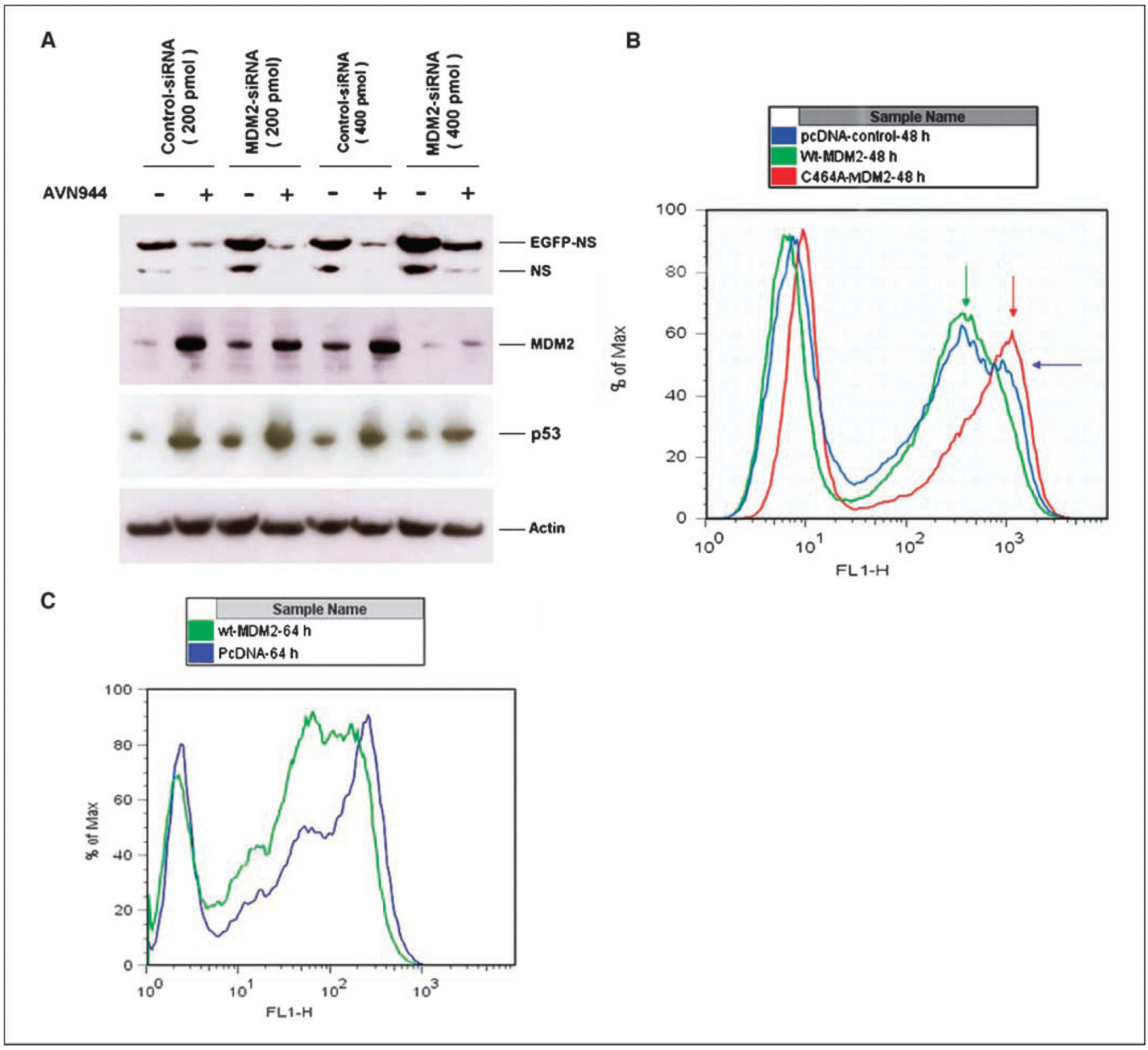

Figure 5.

Effect of Mdm2 siRNA on NS stability in U2OS cells expressing EGFP-NS. *A*, U2OS cells were transiently transfected with 200 or 400 pmol Mdm2-siRNA, control-siRNA, or mock control by Amaxa electroporation. Forty-eight hours after electroporation, AVN944 (1 μmol/L) was added for an additional 16 h, and Western blots for NS, Mdm2, p53, and actin were performed as described in Materials and Methods. *B*, U2OS cells grown in 6-well plates were transiently transfected with pcDNA, wild-type cytomegalovirus-Mdm2 (8 μg), or C464A-Mdm2 (8 μg), the E3-ligase mutant of Mdm2. Forty-eight hours after transfection, quantitative assessment of EGFP-NS protein was performed by flow cytometry and the results shown as a histogram. *Blue line*, the control EGFP-NS expressing U2OS cells; EGFP-NS–expressing U2OS cells in the presence of wt-Mdm2 (*green line*) and C464A-

Mdm2 (red lines), respectively. *C*, U2OS cells grown in 6-well plates were transiently transfected with pcDNA (16 μg) or wild-type CMV-Mdm2 (16 μg). Sixty-four hours after transfection, quantitative assessment of EGFP-NS protein was performed by flow cytometry, and the results shown as a histogram. *Red line*, control EGFP-NS expressing U2OS cells; *green line*, EGFP-NS–expressing U2OS cells in the presence of wt-Mdm2.

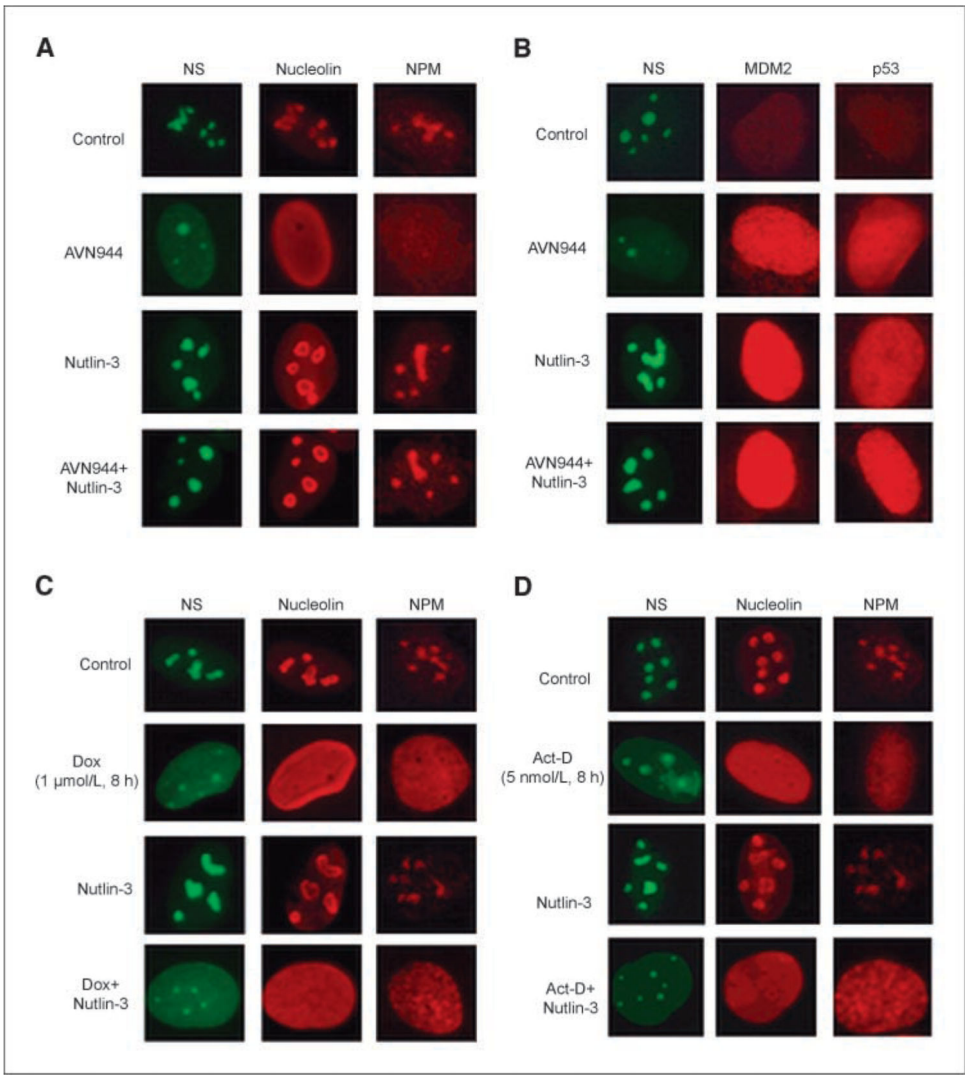

Figure 6.

Pretreatment of U2OS cells with nutlin-3a (24 h) prevents AVN-944–induced translocation of NS, NPM, and nucleolin but fails to prevent Doxorubicin-or Actinomycin-D–induced translocation of these nucleolar proteins. U2OS cells were pretreated with 10 μmol/L nutlin-3 for 24 h, and then exposed to AVN-944 (1 μmol/L), Act-D (5 nmol/L), or doxorubicin (*Dox;* 1 μmol/L) for an additional 16 h (AVN-944) or 8 h (Act-D and doxorubicin). Cells were then fixed, permeabilized, and stained for nucleolin and NPM, as described in Materials and Methods, and observed using fluorescent microscopy at ×100 magnification.

Table 1

Sequences of primer pairs used for RT-PCR analysis

Gene	Primer sequence	Product (bp)
EGFP-NS	5′-agat*ctcgag*atgaaaaggcctaagttaaagaaag-3′ (forward)	1672
	5′-cggt*ggatcc*ccgttacacataatctgtactgaagtc-3′ (reverse)	
NS1	5′-ggcctaagttaaagaaagcaag-3′ (forward)	482
	5′-ctcttctacctgaggacatc-3′ (reverse)	
NS2	5′-gatctggtaccaaaggagaa-3′ (forward)	440
	5′-cttgctggacttcgcagagc-3′ (reverse)	
Cyclin-B1	5′-gttgatactg cctctccaag-3′ (forward)	474
	5′-cttagtataagtgttgtcagtcac-3′ (reverse)	